Special Issue Paper

Mathematical Methods in the Applied Sciences

Received 11 April 2014

Published online in Wiley Online Library

(wileyonlinelibrary.com) DOI: 10.1002/mma.3447
MOS subject classification: 35J05;35Q;65N30;41A60;47H10

A method to build non-scattering perturbations of two-dimensional acoustic waveguides

A. S. Bonnet-Ben Dhia[a*†], E. Lunéville[a], Y. Mbeutcha[a] and S. A. Nazarov[b,c]

Communicated by M. Dauge

We are interested in finding deformations of the rigid wall of a two-dimensional acoustic waveguide, which are not detectable in the far field, as they produce neither reflection nor conversion of propagative modes. A proof of existence of such invisible deformations has been presented in a previous paper. It combines elements of the asymptotic analysis for small deformations and a fixed-point argument. In the present paper, we give a systematic presentation of the method, and we prove that it works for all frequencies except a discrete set. A particular attention is devoted to the practical implementation of the method. The main difficulty concerns the building of a dual family to given oscillating functions. Advantages and limits of the method are illustrated by several numerical results. Copyright © 2015 John Wiley & Sons, Ltd.

Keywords: waveguide; modal analysis; scattering matrix; asymptotic analysis; cloaking; fixed-point algorithm

1. Introduction

There is currently an active research concerning the possibility of realizing cloaking devices, making objects "invisible" for electromagnetic [1], acoustic [2] or water [3] waves. This activity has been intensified by the recent discovery of new metamaterials that could, in principle, help to curve the optical rays, so that the waves get around the obstacle. Besides, some people try to realize cloaking devices with homogeneous materials, the idea being to exploit the effect of topography on the waves. For instance, a specific shape of the bottom of the ocean can be used to make an obstacle ignored by water waves [4, 5]. Our work follows this second approach. The objective is to find a deformation of the rigid wall of an acoustic waveguide, which is not detectable in the far-field at one (or a finite number of) given frequency.

It is well known that in a waveguide, only a finite number of waves (the propagative modes) can propagate at a given frequency. This number N increases with the frequency. An obstacle located in the waveguide will, in general, perturb the propagation, producing reflections and conversions of propagative modes that can be measured in the far-field. These effects are completely summarized by the so-called scattering matrix (a $2N \times 2N$ unitary matrix) whose entries are the complex reflection and transmission coefficients. The obstacle also produces an evanescent field that is only detectable in the near-field. The obstacle is completely undetectable from far-field measurements (we will say for simplicity that the obstacle is then invisible) if it produces neither reflection nor conversion or even phase-shift in the transmission of the modes. Equivalently, all entries of its scattering matrix must vanish, except $2N$ transmission coefficients that must be equal to 1. The main point here is that the invisibility of the obstacle is rigorously equivalent to a finite number of scalar constraints. Then, to find an invisible obstacle, the natural idea is to take a parametrized description of its geometry (and possibly of its internal properties for a penetrable obstacle) and then looking for parameters satisfying the constraints. Of course, the constraints are non-linear functions of the parameters and the existence of a solution is a complicated question. One can already anticipate that this will become harder when increasing the frequency. At least, the number of required parameters will increase with N (and therefore, with the frequency).

The method that we will present in this paper, and whose main features have been introduced in [6], provides a way to find a deformation of the wall of a two-dimensional acoustic waveguide, which is almost invisible, in the sense that it produces neither reflections

[a] *POEMS (UMR 7231 CNRS-INRIA-ENSTA), ENSTA, 828 Boulevard des Maréchaux, 91762 Palaiseau cedex, France*
[b] *Saint Petersburg State University, Universitetsky pr., 28, Peterhof, St. Petersburg, 198504, Russia,*
[c] *St. Petersburg State Polytechnical University, Polytechnicheskaya ul., 29, Saint Petersburg, 195251, Russia*
* *Correspondence to: A. S. Bonnet-Ben Dhia, POEMS (UMR 7231 CNRS-INRIA-ENSTA), ENSTA, 828 Boulevard des Maréchaux, 91762 Palaiseau cedex, France.*
† *E-mail: anne-sophie.bonnet-bendhia@ensta-paristech.fr*

Copyright © 2015 John Wiley & Sons, Ltd.

nor conversions of modes but maybe a phase shift of the modes when they go across the obstacle. We will see later why this phase shift cannot be avoided. More precisely, our method gives a way to choose the parametrization of the shape of the wall, as a linear combination of given shape functions, with a very low number of parameters (exactly $2N^2$), and such that the existence of a solution is ensured; indeed, the constraints are written as a fixed-point equation for a contraction map (in $\mathbb{R}^{2N^2}$). This leads to a natural efficient numerical algorithm. Also, we will see that contrary to a full-numerical shape optimization approach (as proposed in [4]), the method presented here allows to impose a priori features to the invisible obstacle, via the choice of the parametrization. For instance, the user can decide to look for an invisible bump or for an invisible cavity.

The main limitation of our method is that it relies on an asymptotic analysis, and therefore, it works very well for finding small invisible deformations, but may fail for larger ones. Indeed, the contraction property of the fixed point application is directly related to the amplitude ε of the deformation. One objective of the present paper is to quantify this limitation via numerical tests.

The outline of the paper is the following. In Section 2, the theoretical background of the method is recalled. The general multimodal case is presented, extending the asymptotic formulas of [6]. The main result of existence of invisible deformations, as solutions to fixed-point equations, is presented in Section 3. The practical implementation of the method is explained in section 4, with a particular attention devoted to the building of the shape functions. Numerical results are finally presented in Section 5.

2. The theoretical background

2.1. *Scattering matrix and invisibility*

We consider a two-dimensional waveguide occupying the domain $\Omega_0 = \mathbb{R}\times]0,1[$. The homogeneous time-harmonic equations satisfied by the complex valued acoustic pressure $u(x,y)$ read

$$\begin{cases} \Delta u + k^2 u = 0 \text{ in } \Omega_0, \\ \frac{\partial u}{\partial \nu} = 0 \quad \text{on } \partial\Omega_0, \end{cases} \tag{1}$$

where $k = \omega/c > 0$ denotes the wavenumber; ω, the pulsation; and c, the sound speed. The modes are solution of (1) with separated variables. There are two families of modes propagating in opposite directions defined by the following:

$$u_n^{\pm}(x,y) = a_n \cos(n\pi y) e^{\pm i\beta_n x} \text{ for } n \in \mathbb{N}, \tag{2}$$

$$\text{where } \beta_n = \begin{cases} \sqrt{k^2 - n^2\pi^2} & \text{if } k \geq n\pi, \\ i\sqrt{n^2\pi^2 - k^2} & \text{if } k < n\pi, \end{cases} \quad \text{and } a_n = \begin{cases} \frac{1}{\sqrt{k}} & \text{if } n = 0, \\ \frac{\sqrt{2}}{\sqrt{\beta_n}} & \text{if } n > 0. \end{cases} \tag{3}$$

The normalization factor a_n is chosen such that the scattering matrix defined in the succeeding text is unitary. For $k > n\pi$, $\beta_n \in \mathbb{R}$ and the mode is propagative, and for $k < n\pi$, $\beta_n \in i\mathbb{R}$ and the mode is evanescent. The cut-off values $k = n\pi$ will not be considered in the sequel. For a given frequency, and therefore for a given value of k, there exist only a finite number of propagative modes, which will be convenient to denote by $N(k) + 1$, where

$$N(k) = \max\{n \in \mathbb{N}; n\pi < k\}.$$

Now, we consider a locally perturbed waveguide occupying the domain

$$\Omega = \{(x,y); x \in \mathbb{R} \text{ and } 0 < y < 1 + H(x)\},$$

where H is a compactly supported function that describes the deformation of the upper wall of the waveguide (Figure 1). We suppose that H is smooth, in the sense that $H \in W^{2,\infty}(\mathbb{R})$. In other words, H has a continuous derivative and a bounded second derivative (this regularity assumption will be done throughout the whole paper for all shape functions). We are then interested in determining the scattering effects of this deformation on an incident propagative mode u_{inc}. This scattering problem consists in finding u, satisfying

$$\begin{cases} \Delta u + k^2 u = 0 \text{ in } \Omega, \\ \frac{\partial u}{\partial \nu} = 0 \quad \text{on } \partial\Omega, \end{cases} \tag{4}$$

and such that $u - u_{inc}$ is outgoing, in the sense that there exist complex coefficients $\alpha_j^{\pm}$, such that

$$u - u_{inc} = \sum_{j\in\mathbb{N}} \alpha_j^{\pm} u_j^{\pm} \text{ for } x \to \pm\infty. \tag{5}$$

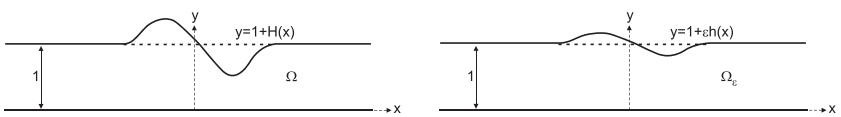

Figure 1. Left: the domain Ω. Right: the domain Ω_ε.

Copyright © 2015 John Wiley & Sons, Ltd.

It is well known that problem (4,5) is well-posed, except maybe for a countable sequence of values of k. For these values, exponentially decaying solutions exist, which are modes trapped by the deformation; then problem (4,5) has a solution defined up to an additive trapped mode. It will be useful in the sequel to rewrite the aforementioned condition (5) by distinguishing two cases, depending on the propagation direction of u_{inc}.

- If $u_{inc} = u_n^+$, with $0 \leq n \leq N(k)$, u satisfies (5) if and only if there exist complex coefficients r_{nj}^- and t_{nj}^+, such that

$$u = \begin{cases} u_n^+ + \sum_{j=0}^{N(k)} r_{nj}^- u_j^- + u_{ev}^- & \text{for } x \to -\infty, \\ \sum_{j=0}^{N(k)} t_{nj}^+ u_j^+ + u_{ev}^+ & \text{for } x \to +\infty, \end{cases} \tag{6}$$

  where $u_{ev}^{\pm}$ are exponentially decaying functions of $|x|$.
- If $u_{inc} = u_n^-$, with $0 \leq n \leq N(k)$, u satisfies (5) if and only if there exist complex coefficients r_{nj}^+ and t_{nj}^-, such that

$$u = \begin{cases} u_n^- + \sum_{j=0}^{N(k)} r_{nj}^+ u_j^+ + u_{ev}^+ & \text{for } x \to +\infty, \\ \sum_{j=0}^{N(k)} t_{nj}^- u_j^- + u_{ev}^- & \text{for } x \to -\infty, \end{cases} \tag{7}$$

  where $u_{ev}^{\pm}$ are exponentially decaying functions of $|x|$.

The coefficients $r_{nj}^{\pm}$ are the reflection coefficients, while the coefficients $t_{nj}^{\pm}$ are the transmission coefficients. All these coefficients are the entries of the so-called scattering matrix **S** defined as follows:

$$\mathbf{S} = \begin{pmatrix} r_{00}^- & r_{01}^- & \cdots & t_{00}^+ & t_{01}^+ & \cdots \\ r_{10}^- & r_{11}^- & \cdots & t_{10}^+ & t_{11}^+ & \cdots \\ \cdots & \cdots & \cdots & \cdots & \cdots & \cdots \\ t_{00}^- & t_{01}^- & \cdots & r_{00}^+ & r_{01}^+ & \cdots \\ t_{10}^- & t_{11}^- & \cdots & r_{10}^+ & r_{11}^+ & \cdots \\ \cdots & \cdots & \cdots & \cdots & \cdots & \cdots \end{pmatrix} \tag{8}$$

This is a matrix of size $\mathcal{N}(k) \times \mathcal{N}(k)$ where $\mathcal{N}(k) = 2(N(k) + 1)$. One can check that **S** is a symmetric unitary matrix [7], and these properties will be extensively used in the sequel.

We can now introduce some definitions:

Definition 1

- The deformation $H(x)$ is said **non reflecting** if $r_{nj}^{\pm} = 0, \forall n, j \in \{0, 1, \cdots N(k)\}$.
- The deformation $H(x)$ is said **non reflecting and non converting** if $r_{nj}^{\pm} = 0 \; \forall n, j \in \{0, 1, \cdots N(k)\}$ and $t_{nj}^{\pm} = 0 \; \forall n, j \in \{0, 1, \cdots N(k)\}$ with $n \neq j$.
- The deformation $H(x)$ is said **invisible up to a phase shift** if $r_{nj}^{\pm} = 0 \; \forall n, j \in \{0, 1, \cdots N(k)\}$, $t_{nj}^{\pm} = 0 \; \forall n, j \in \{0, 1, \cdots N(k)\}$ with $n \neq j$ and $t_{nn}^{\pm} = t_{jj}^{\pm}$, $\forall n, j \in \{0, 1, \cdots N(k)\}$.
- The deformation $H(x)$ is said **invisible** if $r_{nj}^{\pm} = 0$ and $t_{nj}^{\pm} = \delta_{nj}$, $\forall n, j \in \{0, 1, \cdots N(k)\}$.

Clearly, invisibility implies invisibility up to a phase shift, which implies non reflectivity and no conversion, which implies non reflectivity. The four notions have a practical interest, depending on the measures that are available in the experimental setup.

The terminology is quite clear. By canceling the coefficients $r_{nj}^{\pm}$, we ensure the absence of reflections, and by canceling also the coefficients $t_{nj}^{\pm}$ for $n \neq j$, we ensure the absence of conversion between different modes. Then, if the n^{th} propagative mode is incident, no other propagative modes are produced by the presence of the perturbation. Only the amplitude of the mode can take two different values on the two sides of the perturbation. The ratio of these two values is exactly $t_{nn}^{\pm}$ ($\pm$ depending on whether the mode is right or left going). But from the unitary property of the scattering matrix, we know that $|t_{nn}^{\pm}| = 1$, so that $t_{nn}^{\pm} = e^{i\theta_n^{\pm}}$, where $\theta_n^{\pm}$ is the phase shift produced by the perturbation on the nth mode. Now clearly, if $t_{nn}^{\pm} = t_{jj}^{\pm} \forall n, j$, then $\theta_n^{\pm} = \theta_j^{\pm}$, which means that the effect of the perturbation on any linear combination of propagative modes will be only a phase shift.

The properties of the scattering matrix **S** can be exploited to give equivalent reduced statements of the aforementioned definitions. For instance, suppose that $0 < k < \pi$, so that $N(k) = 0$, which means that only the plane mode $n = 0$ is propagating. Then the scattering matrix takes the simple following form:

$$\mathbf{S} = \begin{pmatrix} r_{00}^- & t_{00}^+ \\ t_{00}^- & r_{00}^+ \end{pmatrix}$$

The symmetry gives $t_{00}^+ = t_{00}^-$. The unitary property gives the energy conservation

$$\left|r_{00}^-\right|^2 + \left|t_{00}^+\right|^2 = \left|r_{00}^+\right|^2 + \left|t_{00}^-\right|^2 = 1$$

Copyright © 2015 John Wiley & Sons, Ltd.

and the orthogonality relation:

$$\overline{t_{00}^{-}} r_{00}^{+} = -t_{00}^{+} \overline{r_{00}^{-}}.$$

As a consequence, the simple constraint

$$r_{00}^{-} = 0 \tag{9}$$

implies

$$\left|t_{00}^{+}\right| = \left|t_{00}^{-}\right| = 1 \text{ and } r_{00}^{+} = 0.$$

This shows that when $0 < k < \pi$, the deformation is invisible up to a phase shift (which is equivalent in the single-mode regime to non reflecting and non converting) as soon as the only complex constraint (9) is satisfied. To achieve a perfect invisibility (without phase shift), it is sufficient to impose in addition that $\Re e\left(t_{00}^{+}\right) = 1$ (or alternatively that $\Im m\left(t_{00}^{+}\right) = 0$). Unfortunately, we will explain why this is not possible with our approach.

Let us now discuss the general multimodal case. We have the following result:

Lemma 1
The deformation is non reflecting and non converting as soon as the following $(N(k)+1)^2$ complex constraints are satisfied:

$$\begin{cases} r_{nj}^{-} = 0 \;\; n = 0, \cdots, N(k),\; j = n, \cdots, N(k), \\ t_{nj}^{+} = 0 \;\; n = 0, \cdots, N(k),\; j = n+1, \cdots, N(k). \end{cases} \tag{10}$$

This lemma proves that $(N(k)+1)^2$ complex identities are sufficient to ensure $4(N(k)+1)^2 - 2N(k)$ constraints (1 instead of 4 for $N(k) = 0$, 4 instead of 12 for $N(k) = 1$ etc$\cdots$). If we add to (10) the following $N(k)$ complex conditions

$$t_{nn}^{\pm} = t_{jj}^{\pm},\ \forall n, j \in \{0, 1, \cdots N(k)\},$$

we ensure that there is no conversion, and if moreover

$$\Re e\left(t_{nn}^{+}\right) = 1 \;\text{ for some } n \in \{0, \cdots, N(k)\},$$

perfect invisibility is achieved. But our method does not allow to impose neither of these two last conditions, and we will only build deformations that are non reflecting and non converting.

Proof
Suppose (10) holds. Then the symmetry of the scattering matrix **S** implies that $r_{nj}^{-} = 0$ for all n and j. Thus, we can suppose now that

$$\begin{cases} r_{nj}^{-} = 0 \;\; n = 0, \cdots, N(k),\; j = 0, \cdots, N(k), \\ t_{nj}^{+} = 0 \;\; n = 0, \cdots, N(k),\; j = n+1, \cdots, N(k). \end{cases} \tag{11}$$

Taking in particular $n = 0$, we see that all the coefficients of the first line of **S** vanish, except t_{00}^{+}. Since **S** is a unitary matrix, this coefficient is necessary such that $\left|t_{00}^{+}\right| = 1$. Then, again, by unitarity of **S**, all coefficients in the same row as t_{00}^{+} must vanish:

$$\begin{cases} t_{j0}^{+} = 0 \;\; j = 1, \cdots, N(k), \\ r_{j0}^{+} = 0 \;\; j = 0, \cdots, N(k). \end{cases} \tag{12}$$

Now, taking $n = 1$ in (11) and using (12), we see that all the coefficients of the second line of **S** vanish, except t_{11}^{+}, so that $\left|t_{11}^{+}\right| = 1$. We can then continue the process and prove the lemma step by step. □

2.2. *The asymptotic analysis*

Now, the idea is to consider a small deformation of the form $H(x) = \varepsilon h(x)$, where h is a smooth compactly supported function and ε, a small parameter (Figure 1), so that an asymptotic procedure can be carried. We do not present here the details of the calculations (which are given in [6] and rely on the theory of [8]), but we give a precise statement of the main result. For ε small enough, we denote by Ω_ε the new connected domain defined by:

$$\Omega_\varepsilon = \{(x, y); x \in \mathbb{R} \text{ and } 0 < y < 1 + \varepsilon h(x)\}$$

and by $r_{nj}^{\pm}(\varepsilon)$ and $t_{nj}^{\pm}(\varepsilon)$, the corresponding scattering coefficients. One can establish an asymptotic expansion of these scattering coefficients. To give the result, we need the following definition. For $k > n\pi$, we denote by v_n^{+} the unique outgoing solution of the following problem:

$$\begin{cases} \Delta v_n^{+} + k^2 v_n^{+} = 0 & \text{in} \quad \Omega_0, \\ \frac{\partial v_n^{+}}{\partial y} = 0 & \text{on} \quad \{y = 0\}, \\ \frac{\partial v_n^{+}}{\partial y} = g_n^{+} & \text{on} \quad \{y = 1\}, \end{cases} \tag{13}$$

Copyright © 2015 John Wiley & Sons, Ltd.

where

$$g_n^+(x) = \frac{dh}{dx}(x)\frac{\partial u_n^+}{\partial x}(x,1) + n^2\pi^2 h(x) u_n^+(x,1).$$

Notice that since h is compactly supported, g_n^+ is also compactly supported and that is why v_n^+ admits a modal expansion for x large enough. Since, moreover, v_n^+ is outgoing, there exist complex coefficients R_{nj}^- and T_{nj}^+, such that

$$v_n^+ = \begin{cases} \sum_{j=0}^{N(k)} R_{nj}^- u_j^- + v_{ev}^- & \text{for } x \to -\infty, \\ \sum_{j=0}^{N(k)} T_{nj}^+ u_j^+ + v_{ev}^+ & \text{for } x \to +\infty, \end{cases} \tag{14}$$

where $v_{ev}^{\pm}$ are exponentially decaying functions of $|x|$. Then we have

Theorem 1
The scattering coefficients $r_{nj}^-(\varepsilon)$ and $t_{nj}^+(\varepsilon)$ for $n, j = 0, \cdots, N(k)$ admit the following expansion

$$\begin{cases} r_{nj}^-(\varepsilon) = \varepsilon R_{nj}^- + \varepsilon^2 \tilde{R}_{nj}^-, \\ t_{nj}^+(\varepsilon) = \delta_{nj} + \varepsilon T_{nj}^+ + \varepsilon^2 \tilde{T}_{nj}^+, \end{cases} \tag{15}$$

where $\tilde{R}_{nj}^-$ and $\tilde{T}_{nj}^-$ are bounded functions of ε and δ_{nj} denotes the Kronecker delta.

Let us now derive explicit expressions of the first order terms of the scattering coefficients R_{nj}^- and T_{nj}^+.

Lemma 2
For $n, j = 0, \cdots, N(k)$:

$$\begin{cases} R_{nj}^- = \frac{i}{2}(-1)^{n+j} a_n a_j \left(k^2 + \beta_n \beta_j\right) \int_{\mathbb{R}} h(x) e^{i(\beta_n + \beta_j)x} dx, \\ T_{nj}^+ = \frac{i}{2}(-1)^{n+j} a_n a_j \left(k^2 - \beta_n \beta_j\right) \int_{\mathbb{R}} h(x) e^{i(\beta_n - \beta_j)x} dx, \end{cases} \tag{16}$$

where a_n and β_n have been defined by (3).

Proof
Let us introduce the rectangle $Q_L =]-L, L[\times]0,1[$. For L large enough, we can assume that $h(x) = 0$ if $|x| > L$. Then, since v_n^+ defined by (13) and the modes $u_j^{\pm}$ satisfy the homogeneous Helmholtz equation in Q_L, the following Green formula holds:

$$\int_{\partial Q_L} \frac{\partial v_n^+}{\partial \nu} \overline{u_j^{\pm}} - \overline{\frac{\partial u_j^{\pm}}{\partial \nu}} v_n^+ = 0.$$

Since v_n^+ and $u_j^{\pm}$ satisfy Neumann boundary conditions on the boundaries $y = 0$ and $y = 1$, the previous equality can be rewritten:

$$\int_{\Sigma_L^- \cup \Sigma_L^+} \frac{\partial v_n^+}{\partial \nu} \overline{u_j^{\pm}} - \overline{\frac{\partial u_j^{\pm}}{\partial \nu}} v_n^+ + \int_{\mathbb{R}} g_n^+(x) \overline{u_j^{\pm}(x,1)} dx = 0, \tag{17}$$

where $\Sigma_L^{\pm} = \{\pm L\}\times]0,1[$. Then using the modal expansion of v_n^+ and the orthogonality between the modes on the cross-section of the guide, we obtain

$$\int_{\Sigma_L^-} \frac{\partial v_n^+}{\partial \nu} \overline{u_j^{\pm}} - \overline{\frac{\partial u_j^{\pm}}{\partial \nu}} v_n^+ = i(1 \mp 1) R_{nj}^- \quad \text{and} \quad \int_{\Sigma_L^+} \frac{\partial v_n^+}{\partial \nu} \overline{u_j^{\pm}} - \overline{\frac{\partial u_j^{\pm}}{\partial \nu}} v_n^+ = i(1 \pm 1) T_{nj}^+. \tag{18}$$

On the other hand, integrating by parts gives

$$\int_{\mathbb{R}} g_n^+(x) \overline{u_j^{\pm}(x,1)} dx = \int_{\mathbb{R}} h(x) \left(-\frac{d}{dx} \left(\frac{\partial u_n^+}{\partial x}(x,1) \overline{u_j^{\pm}}(x,1) \right) + n^2\pi^2 u_n^+(x,1) \overline{u_j^{\pm}}(x,1) \right) dx,$$

which can be simplified in

$$\int_{\mathbb{R}} g_n^+(x) \overline{u_j^{\pm}(x,1)} dx = \left(k^2 \mp \beta_n \beta_j\right) a_n a_j (-1)^{n+j} \int_{\mathbb{R}} h(x) e^{i(\beta_n \mp \beta_j)x} dx. \tag{19}$$

The lemma follows by combining (17), (18), and (19). □

Let us comment the previous result.

First, notice that considering the scattering matrix as a function of H, we could use the notation $r_{nj}^-(H + \varepsilon h)|_{H=0}$ instead of $r_{nj}^-(\varepsilon)$, and the same for $t_{nj}^+(\varepsilon)$. Then it appears clearly that the formulas (16) define linear forms of h, which are exactly the Fréchet derivatives of r_{nj}^- and t_{nj}^+ computed at $H = 0$.

Copyright © 2015 John Wiley & Sons, Ltd.

In particular, the previous lemma gives a way to choose $h(x)$ in the kernel of these derivatives. For instance, if h is such that

$$\int_{\mathbb{R}} h(x)e^{j(\beta_n \pm \beta_j)x}dx = 0 \quad \forall n, j = 0, \cdots, N(k),$$

then, combining Lemma 2 and Theorem 1, we see that a deformation of the form $y = 1 + \varepsilon h(x)$ will produce a scattered field that is at most of order ε^2.

Suppose on the contrary that for some $n, j \in \{0, \cdots, N(k)\}$, we find h such that (for instance) $R^-_{nj} = 1$. Then by Theorem 1, we can say that the real part of the coefficient $r^-_{nj}(\varepsilon)$ takes strictly positive values for small ε. On the other hand, if we change h in $-h$, it takes strictly negative values for small ε. If we can also prove that the imaginary part of $r^-_{nj}(\varepsilon)$ takes positive and negative values for small deformations, we are inclined to assume that $r^-_{nj}(\varepsilon)$ can vanish (not only at $H = 0$ but also on a variety in the space of H functions), and we will indeed prove this result later.

Looking further at formulas (16), we can notice that

$$T^+_{00} = 0.$$

This means that the effect of the deformation on the transmission of the fundamental mode $n = 0$ is always of order ε^2. This is a good news if we just want to obtain invisibility at the first order in ε for some $k < \pi$. But for our purpose, which is to get perfect invisibility, it is definitely not a good news. Indeed, this means that a priori neither the real part nor the imaginary part of $t^+_{00}(\varepsilon)$ could change its sign. Then it is possible that t^+_{00} does not vanish, except at $H = 0$. That is why we cannot ensure the perfect invisibility with our method.

More generally, we can notice that $T^+_{nn} = 0$ for all $n = 1, \cdots, N(k)$ as soon as

$$\int_{\mathbb{R}} h(x)dx = 0.$$

Again, this is a very good news if we just want to obtain invisibility at the first order in ε since one single constraint on h (a zero mean value) is sufficient to ensure that $t^+_{nn} - 1$ is of order ε^2 for all $n = 1, \cdots, N(k)$. But on the other hand, this means that the Fréchet derivative of the application $H \longmapsto \left(t^+_{00}, \cdots, t^+_{N(k)N(k)}\right)$ is degenerate, and this is the reason why we cannot build perfectly invisible deformations, nor deformations invisible up to a phase shift, when $k > \pi$.

3. The fixed point equation

3.1. *The single-mode case*

Let us begin with the single-mode case that corresponds to $0 < k < \pi$ an $N(k) = 0$. As explained previously, the deformation $y = 1 + \varepsilon h(x)$ is invisible up to a phase shift if and only if (9) holds, i.e., with the notations of Theorem 1, $r^-_{00}(\varepsilon) = 0$. Then using (15) and Lemma 2, we can equivalently say that the deformation $y = 1 + \varepsilon h(x)$ is invisible up to a phase shift if and only if

$$R^-_{00} + \varepsilon \tilde{R}^-_{00} = 0 \tag{20}$$

where

$$R^-_{00} = ik \int_{\mathbb{R}} h(x)e^{2ikx}dx \tag{21}$$

and where $\tilde{R}^-_{00}$ is the rest in (15).

Now, we look for a solution h of (20) of the following form:

$$h = h_0 + \hat{\tau}\hat{h} + \check{\tau}\check{h}, \tag{22}$$

where $\hat{\tau}$ and $\check{\tau}$ are unknown real parameters and h_0, $\hat{h}$, and $\check{h}$ are a priori chosen functions such that $h_0 \neq 0$ and

$$\begin{aligned} &\textstyle\int_{\mathbb{R}} h_0(x)\cos(2kx)dx = 0 \quad \text{and} \quad \int_{\mathbb{R}} h_0(x)\sin(2kx)dx = 0, \\ &\textstyle\int_{\mathbb{R}} \hat{h}(x)\cos(2kx)dx = 1 \quad \text{and} \quad \int_{\mathbb{R}} \hat{h}(x)\sin(2kx)dx = 0, \\ &\textstyle\int_{\mathbb{R}} \check{h}(x)\cos(2kx)dx = 0 \quad \text{and} \quad \int_{\mathbb{R}} \check{h}(x)\sin(2kx)dx = 1. \end{aligned} \tag{23}$$

Let us emphasize that it is indeed possible to find smooth compactly supported functions h_0, $\hat{h}$ and $\check{h}$ satisfying (23). There are even many possibilities for that, which will be discussed in the next section. Notice also that such functions h_0, $\hat{h}$ and $\check{h}$ are necessarily linearly independent (otherwise they would not satisfy (23)) so that h given by (22) cannot be equal to 0.

Plugging (22) and (23) into (20), we obtain the following equation for $\tau = \hat{\tau} + i\check{\tau}$:

$$ik\tau + \varepsilon \tilde{R}^-_{00} = 0,$$

which can be rewritten

$$\tau = F(\varepsilon, \tau) \tag{24}$$

Copyright © 2015 John Wiley & Sons, Ltd.

with

$$F(\varepsilon,\tau) = \frac{i\varepsilon}{k}\tilde{R}_{00}^{-},$$

where $\tilde{R}_{00}^{-}$ is the rest in (15) associated to the profile

$$y = 1 + \varepsilon\left(h_0(x) + \hat{\tau}\hat{h}(x) + \check{\tau}\check{h}(x)\right).$$

The existence of a solution to (24) is finally given by

Theorem 2
For $0 < k < \pi$, let $h_0 \neq 0, \hat{h}$ and $\check{h}$ denote smooth and compactly supported functions satisfying (23). Then for ε small enough, there exists a unique $\tau = \hat{\tau} + i\check{\tau} \in \mathbb{C}$ such that the deformation $y = 1 + \varepsilon(h_0(x) + \hat{\tau}\hat{h}(x) + \check{\tau}\check{h}(x))$ is invisible up to a phase shift.

Proof
We give here only the main arguments of the proof (see [6] and [9] for details). First, we use the change of variables

$$(x,y) \to \left(x, \frac{y}{1+\varepsilon h(x)}\right) \tag{25}$$

to set the problem in a straight waveguide $\Omega_0 = \mathbb{R}\times]0,1[$. Thanks to this rectification; the scattering problem originally set in the homogeneous deformed waveguide is rewritten as a scattering problem in a heterogeneous straight waveguide; the coefficients $\varepsilon, \varepsilon\hat{\tau}$ and $\varepsilon\check{\tau}$ then appearing in the coefficients of the partial differential equation. This allows to prove that the scattering coefficients $r_{nj}^{\pm}(\varepsilon)$ and $t_{nj}^{\pm}(\varepsilon)$, and in particular $r_{00}^{-}(\varepsilon)$, are analytic functions of $(\varepsilon, \hat{\tau}, \check{\tau})$. Moreover, by Theorem 1, the function

$$\tilde{R}_{00}^{-} = \frac{r_{00}^{-}(\varepsilon) - \varepsilon R_{00}^{-}}{\varepsilon^2}$$

is bounded for bounded ε and τ. As a consequence, there exists $\varepsilon_0 > 0, \rho_0 > 0$ and a constant C, such that for any $\varepsilon \leq \varepsilon_0, |\tau| < \rho_0$ and $|\tau'| < \rho_0$

$$\begin{aligned} &|F(\varepsilon,\tau)| \leq \rho_0, \\ &|F(\varepsilon,\tau) - F(\varepsilon,\tau')| \leq C\varepsilon|\tau - \tau'|. \end{aligned} \tag{26}$$

This proves that the mapping $\tau \to F(\varepsilon,\tau)$ is a contraction in the ball $|\tau| < \rho_0$ for ε small enough. The result follows classically by the fixed-point theorem. □

3.2. *The multi-frequency case*

The previous result can be easily extended to the multi-frequency case. The objective is to find a deformation of the wall of the waveguide, which is invisible up to a phase shift at M frequencies ($M > 1$) associated to the wavenumbers $0 < k_1 < k_2 \cdots < k_M < \pi$. Proceeding as previously, we state that the deformation $y = 1 + \varepsilon h(x)$ is invisible up to a phase shift if and only if

$$R_{00}^{-}(k_m) + \varepsilon\tilde{R}_{00}^{-}(k_m) = 0 \quad \forall m = 1, 2\cdots M, \tag{27}$$

where

$$R_{00}^{-}(k_m) = ik_m \int_{\mathbb{R}} h(x) e^{2ik_m x} dx, \tag{28}$$

and where $\tilde{R}_{00}^{-}(k_m)$ is the rest in (15) for $k = k_m$. The method then requires the introduction of $2M+1$ shape functions $h_0 \neq 0, \hat{h}_j$ and $\check{h}_j, j = 1, 2\cdots M$, such that

$$\begin{aligned} &\textstyle\int_{\mathbb{R}} h_0(x)\cos(2k_m x)dx = 0 \quad \text{and} \quad \int_{\mathbb{R}} h_0(x)\sin(2k_m x)dx = 0, \quad m = 1, 2\cdots M, \\ &\textstyle\int_{\mathbb{R}} \hat{h}_j(x)\cos(2k_m x)dx = \delta_{mj} \quad \text{and} \quad \int_{\mathbb{R}} \hat{h}_j(x)\sin(2k_m x)dx = 0, \quad j, m = 1, 2\cdots M, \\ &\textstyle\int_{\mathbb{R}} \check{h}_j(x)\cos(2k_m x)dx = 0 \quad \text{and} \quad \int_{\mathbb{R}} \check{h}_j(x)\sin(2k_m x)dx = \delta_{mj}, \; j, m = 1, 2\cdots M. \end{aligned} \tag{29}$$

The existence of shape functions $h_0 \neq 0, \hat{h}_j$ and $\check{h}_j, j = 1, 2\cdots M$, satisfying (29) is a simple result of linear algebra that will be detailed in Subsection 4.1. Then we can prove exactly as in the single-frequency case the following theorem:

Theorem 3
For $0 < k_1 < k_2 \cdots < k_M < \pi$, let $h_0, \hat{h}_j$ and $\check{h}_j, j = 1, 2\cdots M$, denote smooth and compactly supported functions satisfying (29). Then for ε small enough, there exists a unique $\tau = (\hat{\tau}_1 + i\check{\tau}_1, \hat{\tau}_2 + i\check{\tau}_2, \cdots \hat{\tau}_M + i\check{\tau}_M)$ in $\mathbb{C}^M$ such that the deformation

$$y = 1 + \varepsilon\left(h_0(x) + \sum_{j=1}^{M} \hat{\tau}_j\hat{h}_j(x) + \sum_{j=1}^{M} \check{\tau}_j\check{h}_j(x)\right)$$

Copyright © 2015 John Wiley & Sons, Ltd.

is invisible up to a phase shift.

3.3. *The multimodal case*

More intricate is the search of a deformation that is non reflecting and non converting at a frequency greater than π, when several modes are propagating. The generalization to a multifrequency multimodal case is possible, but for the sake of clarity, the presentation here is restricted to one frequency.

Let $k > 0$ such that $N(k) > 0$. From Lemma 1, Theorem 1, and Lemma 2, we deduce that the deformation $y = 1 + \varepsilon h(x)$ is invisible up to a phase shift if and only if

$$\begin{aligned} R_{nj}^- + \varepsilon \tilde{R}_{nj}^- &= 0 \; n = 0, \cdots, N(k), \; j = n, \cdots, N(k), \\ T_{nj}^+ + \varepsilon \tilde{T}_{nj}^+ &= 0 \; n = 0, \cdots, N(k), \; j = n+1, \cdots, N(k), \end{aligned} \tag{30}$$

where

$$R_{nj}^- = \alpha_{nj}^+ \int_{\mathbb{R}} h(x) e^{i(\beta_n + \beta_j)x} dx \text{ and } T_{nj}^+ = \alpha_{nj}^- \int_{\mathbb{R}} h(x) e^{i(\beta_n - \beta_j)x} dx \tag{31}$$

with

$$\alpha_{nj}^{\pm} = \frac{i}{2}(-1)^{n+j} a_n a_j \left(k^2 \pm \beta_n \beta_j\right),$$

and where $\tilde{R}_{nj}^-$ and $\tilde{T}_{nj}^+$ are the rests in (15).

Proceeding as previously, the idea is to look for a solution h of (30) of the following form:

$$h = h_0 + \sum_{n=0}^{N(k)} \sum_{j=n}^{N(k)} \left(\hat{\tau}_{nj}^+ \hat{h}_{nj}^+ + \check{\tau}_{nj}^+ \check{h}_{nj}^+ \right) + \sum_{n=0}^{N(k)} \sum_{j=n+1}^{N(k)} \left(\hat{\tau}_{nj}^- \hat{h}_{nj}^- + \check{\tau}_{nj}^- \check{h}_{nj}^- \right), \tag{32}$$

where the $\hat{\tau}_{nj}^{\pm}$ and $\check{\tau}_{nj}^{\pm}$ are $2(N(k)+1)^2$ unknown real parameters and h_0, $\hat{h}_{nj}^{\pm}$ and $\check{h}_{nj}^{\pm}$ are a priori chosen functions such that

$$\begin{aligned} &\int_{\mathbb{R}} h_0(x) \cos((\beta_n + \beta_j)x) dx = 0 \text{ and } \int_{\mathbb{R}} h_0(x) \sin((\beta_n + \beta_j)x) dx = 0, n = 0, \cdots, N(k), \; j = n, \cdots, N(k), \\ &\int_{\mathbb{R}} h_0(x) \cos((\beta_n - \beta_j)x) dx = 0 \text{ and } \int_{\mathbb{R}} h_0(x) \sin((\beta_n - \beta_j)x) dx = 0, n = 0, \cdots, N(k), \; j = n+1, \cdots, N(k), \end{aligned} \tag{33}$$

and

$$\begin{aligned} &\int_{\mathbb{R}} \hat{h}_{nj}^+(x) \cos((\beta_m + \beta_\ell)x) dx = \delta_{mn}\delta_{j\ell} \text{ and } \int_{\mathbb{R}} \hat{h}_{nj}^+(x) \sin((\beta_m + \beta_\ell)x) dx = 0, n = 0, \cdots, N(k), \; j = n, \cdots, N(k), \\ &\int_{\mathbb{R}} \check{h}_{nj}^+(x) \cos((\beta_m + \beta_\ell)x) dx = 0 \text{ and } \int_{\mathbb{R}} \check{h}_{nj}^+(x) \sin((\beta_m + \beta_\ell)x) dx = \delta_{mn}\delta_{j\ell}, n = 0, \cdots, N(k), \; j = n, \cdots, N(k), \\ &\int_{\mathbb{R}} \hat{h}_{nj}^-(x) \cos((\beta_m - \beta_\ell)x) dx = \delta_{mn}\delta_{j\ell} \text{ and } \int_{\mathbb{R}} \hat{h}_{nj}^-(x) \sin((\beta_m - \beta_\ell)x) dx = 0, n = 0, \cdots, N(k), \; j = n+1, \cdots, N(k), \\ &\int_{\mathbb{R}} \check{h}_{nj}^-(x) \cos((\beta_m - \beta_\ell)x) dx = 0 \text{ and } \int_{\mathbb{R}} \check{h}_{nj}^-(x) \sin((\beta_m - \beta_\ell)x) dx = \delta_{mn}\delta_{j\ell}, n = 0, \cdots, N(k), \; j = n+1, \cdots, N(k). \end{aligned} \tag{34}$$

Contrary to the single-mode case, it is not always possible to find functions $\hat{h}_{nj}^{\pm}$ and $\check{h}_{nj}^{\pm}$ satisfying (34). Indeed, this is possible if and only if the functions $x \longmapsto e^{i(\beta_n \pm \beta_j)x}$ are linearly independent, which fails for some values of k. More precisely, let us define the set

$$\mathcal{E}(k) = \{\beta_n + \beta_j; n = 0, \cdots, N(k), \; j = n, \cdots, N(k)\} \cup \{\beta_n - \beta_j; n = 0, \cdots, N(k), \; j = n+1, \cdots, N(k)\}. \tag{35}$$

We have the

Lemma 3

- Let $k > 0$ such that $N(k) > 0$. Then there exist smooth compactly supported functions $\hat{h}_{nj}^{\pm}$, $n = 0, \cdots, N(k)$, $j = n, \cdots, N(k)$, and $\check{h}_{nj}^{\pm}$, $n = 0, \cdots, N(k)$, $j = n+1, \cdots, N(k)$, satisfying (34) if and only if the following condition holds:

$$\text{The cardinal of the set } \mathcal{E}(k) \text{ is equal to } (N(k)+1)^2. \tag{36}$$

- The values of $k > 0$ such that (36) does not hold form an infinite countable set.

Copyright © 2015 John Wiley & Sons, Ltd.

Proof
First, notice that the cardinal of $\{n=0,\cdots,N(k), j=n+1,\cdots,N(k)\}\cup\{n=0,\cdots,N(k), j=n+1,\cdots,N(k)\}$ is equal to $(N(k)+1)^2$, so that the cardinal of $\mathcal{E}(k)$ is always less or equal to $(N(k)+1)^2$. The equality holds if and only if all values $\beta_n \pm \beta_j$ are distinct. Then, using Lemma 4, this proves the first item because it is well known that the functions $x \longmapsto e^{i\gamma_n x}$, for $n = 1, 2\cdots$ are linearly independent if and only if the coefficients γ_n are all distinct.

From the analyticity properties of the functions $k \longmapsto \sqrt{k^2-n^2\pi^2}$ outside the thresholds, and using the fact that the zeros of an analytic function are isolated, we deduce that the values of k such that (36) does not hold (which correspond to intersections of the functions $k \longmapsto \beta_n \pm \beta_j$) form at most a countable set. Finally, one can check that the increasing function $k \longmapsto 2\beta_{N(k)}$ and the decreasing function $k \longmapsto \beta_0 - \beta_1$ have exactly one intersection in the interval $]N(k)\pi, (N(k)+1)\pi[$. This proves that there is indeed an infinite set of values of k such that (36) does not hold. □

Now we can conclude as in the previous cases:

Theorem 4
Let $k > 0$ such that (36) holds and let $h_0 \neq 0, \hat{h}^{\pm}_{nj}, n = 0,\cdots,N(k), j = n,\cdots,N(k)$, and $\check{h}^{\pm}_{nj}, n = 0,\cdots,N(k), j = n+1,\cdots,N(k)$, denote smooth compactly supported functions satisfying (33) and (34). Then for ε small enough, there exists a unique (τ^+,τ^-) in $\mathbb{C}^{(N(k)+1)^2}$ with $\tau^+ = \hat{\tau}^+_{nj} + i\check{\tau}^+_{nj}$ and $\tau^- = \hat{\tau}^-_{nj} + i\check{\tau}^-_{nj}$, such that the deformation

$$y = 1 + \varepsilon\left(h_0 + \sum_{n=0}^{N(k)}\sum_{j=n}^{N(k)}\left(\hat{\tau}^+_{nj}\hat{h}^+_{nj} + \check{\tau}^+_{nj}\check{h}^+_{nj}\right) + \sum_{n=0}^{N(k)}\sum_{j=n+1}^{N(k)}\left(\hat{\tau}^-_{nj}\hat{h}^-_{nj} + \check{\tau}^-_{nj}\check{h}^-_{nj}\right)\right)$$

is non reflecting and non converting.

4. The numerical implementation

Let us now present the main ingredients of the numerical method. On one hand, we need to choose and compute shape functions $h_0, \hat{h}$ and $\check{h}$. This crucial step is discussed in Subsection 4.1. On the other hand, we need a numerical method to compute the scattering coefficients for a given shape of the boundary. This can be done by any available method and could be presented as a black box in the present paper. However, we think that the multimodal approach that we use has some advantages in the present context, compared with finite elements for instance, and it is briefly described in Subsection 4.2 for the sake of completeness. Then we are able to implement the classical fixed-point algorithm presented in Subsection 4.3.

4.1. *The computation of the shape functions*

The construction of the shape functions $h_0, \hat{h}_{\cdots}$ and $\check{h}_{\cdots}$ can be reformulated in the following general setting. Let V denotes an infinite dimensional vectorial space of compactly supported functions of $W^{2,\infty}(\mathbb{R})$, and let $\ell_j, j = 1,\cdots J$, denote J linear forms on V. We look for $(J+1)$ functions $h_j \in V, j = 0,\cdots,J$, such that:

$$\ell_j(h_0) = 0 \text{ and } \ell_i(h_j) = \delta_{ij} \text{ for } i,j = 1,\cdots,J. \tag{37}$$

The existence of (infinitely many) families of functions $(h_j)_{j=0,\cdots J}$ is given by the

Lemma 4
Let V be an infinite dimensional vectorial space and $\ell_j, j = 1,\cdots J$, denote J linear forms on V.

(1) There exists a dual family (h_j) of the family (ℓ_j) (i.e., J elements $h_j \in V, j = 1,\cdots,J$, such that $\ell_i(h_j) = \delta_{ij}$ for $i,j = 1,\cdots,J$) if and only if the linear forms ℓ_j are linearly independent.
(2) The vectorial space $W = \{h \in V; \ell_j(h) = 0,\ \forall j = 1,\cdots J\}$ is infinite dimensional.
(3) If the linear forms (ℓ_j) are linearly independent and if (h_j) denotes a dual family of the (ℓ_j), then $\left(\tilde{h}_j\right)$ is a dual family of the (ℓ_j) if and only if $\tilde{h}_j - h_j \in W$ for all $j = 1,\cdots J$. Besides,

$$W = \left\{h - \sum_{j=1}^{J}\ell_j(h)h_j; h \in V\right\}.$$

(4) Let V_J denotes a subspace of V of dimension J. Then there exists a dual family (h_j) of the family (ℓ_j) with $h_j \in V_J$ if and only if

$$V_J \cap W = \{0\}. \tag{38}$$

Proof
The first item is a standard result of linear algebra (see [10], lemma 4.13). Then, for every $h \in V$, we have $h - \sum_{j=1}^{J}\ell_j(h)h_j \in W$, which proves the second item. The third one is straightforward. To prove the last item, we consider the linear application $\mathcal{T}$ form V_J to $\mathbb{R}^J$ defined by

$$\mathcal{T}(h) = (\ell_1(h),\cdots,\ell_J(h)).$$

Copyright © 2015 John Wiley & Sons, Ltd.

The existence of a dual family in V_J holds if and only if $\mathcal{T}$ is onto, which holds if and only if $\mathcal{T}$ is injective. And by definition, $\mathcal{T}$ is injective if and only if $V_J \cap W = \{0\}$. □

From this lemma, it results that if condition (36) holds, then there exist smooth compactly supported functions $\hat{h}^{\pm}_{nj}$, $n = 0, \cdots, N(k)$, $j = n, \cdots, N(k)$, and $\check{h}^{\pm}_{nj}$, $n = 0, \cdots, N(k), j = n+1, \cdots, N(k)$, satisfying (34), and there are infinitely many possible choices. In accordance with the last item of the lemma, a method to build one particular dual basis is to choose a finite dimensional space (of polynomial functions or spline functions for instance), which has the right dimension. Then if condition (38) holds, which is not easy to know a priori, the computation of the dual basis amounts to solve a linear system.

From a practical point of view, we consider that the best choices are those who lead to 'simple' shapes (a notion that has no clear mathematical definition), which can be realized and reproduced, and such that the fixed-point equation is contractant for an ε, which is not too small. Of course, this will become harder to achieve when the number J of constraints increases (in particular when the frequency increases).

A natural way to reduce the number of constraints is to exploit the parity properties of cos and sin functions. More precisely, we will choose even functions for h_0 and for the $\hat{h}$, and odd functions for the $\check{h}$. Then (33) and (34) reduce to:

$$\begin{aligned}
&\int_{\mathbb{R}} h_0(x)\cos((\beta_n+\beta_j)x)dx = 0, n = 0, \cdots, N(k),\ j = n, \cdots, N(k),\\
&\int_{\mathbb{R}} h_0(x)\cos((\beta_n-\beta_j)x)dx = 0, n = 0, \cdots, N(k),\ j = n+1, \cdots, N(k),
\end{aligned} \tag{39}$$

and

$$\begin{aligned}
&\int_{\mathbb{R}} \hat{h}^{+}_{nj}(x)\cos((\beta_m+\beta_\ell)x)dx = \delta_{mn}\delta_{j\ell}, n = 0, \cdots, N(k),\ j = n, \cdots, N(k),\\
&\int_{\mathbb{R}} \check{h}^{+}_{nj}(x)\sin((\beta_m+\beta_\ell)x)dx = \delta_{mn}\delta_{j\ell}, n = 0, \cdots, N(k),\ j = n, \cdots, N(k),\\
&\int_{\mathbb{R}} \hat{h}^{-}_{nj}(x)\cos((\beta_m-\beta_\ell)x)dx = \delta_{mn}\delta_{j\ell}, n = 0, \cdots, N(k),\ j = n+1, \cdots, N(k),\\
&\int_{\mathbb{R}} \check{h}^{-}_{nj}(x)\sin((\beta_m-\beta_\ell)x)dx = \delta_{mn}\delta_{j\ell}, n = 0, \cdots, N(k),\ j = n+1, \cdots, N(k).
\end{aligned} \tag{40}$$

4.2. *The discretization of the scattering problem*

At each iteration of the fixed-point algorithm, which is described in the next paragraph, one has to evaluate numerically several scattering coefficients for a given shape $y = 1 + \varepsilon h(x)$. We use for that the multimodal method presented in section 3.3 of [11]. Contrary to a 2D finite elements method, the multimodal approach avoids remeshing at each iteration.

Suppose that h is a smooth function, compactly supported in some interval $]-L, L[$ with $L > 0$.

On the one hand, we use again the change of variables (25) to set the initial problem in a straight waveguide $\Omega_0 = \mathbb{R}\times]0,1[$. On the other hand, exact transparent boundary conditions are imposed on the artificial boundaries $x = \pm L$ to write a formulation in the bounded domain $B_L =]-L, L[\times]0,1[$. These transparent conditions are expressed thanks to the so-called Dirichlet-to-Neumann maps of the semi-infinite waveguides $]-\infty, -L[\times]0,1[$ and $]L, +\infty[\times]0,1[$. This leads finally to the following variational problem :

Find $u \in H^1(B_L)$ such that $\forall v \in H^1(B_L)$

$$\int_{B_L}(\mathbb{H}_\varepsilon \nabla u)\cdot\overline{\nabla v} - k^2\int_{B_L}(1+\varepsilon h(x))u\bar{v} - \langle \mathbb{T}_L^{-}u, v\rangle - \left\langle \mathbb{T}_L^{+}u, v\right\rangle = \mathcal{L}_L^{-}(v) + \mathcal{L}_L^{+}(v)$$

$$\mathbb{H}_\varepsilon = \begin{bmatrix} 1+\varepsilon h(x) & -y\varepsilon\frac{dh}{dx}(x) \\ -y\varepsilon\frac{dh}{dx}(x) & \left(1+y^2\varepsilon^2\frac{dh}{dx}(x)^2\right)\frac{1}{1+\varepsilon h(x)} \end{bmatrix}, \tag{41}$$

where the Dirichlet-to-Neumann operators $\mathbb{T}_L^{\pm}$ are defined (with the notations of paragraph 2.1) by: $\left\langle \mathbb{T}_L^{\pm}u, v\right\rangle = \sum_{n\geq 0} i\beta_n u_n(\pm L)\overline{v_n}(\pm L)$ with $u_n(X) = a_n\sqrt{\beta_n}\int_0^1 u(x,y)\cos(n\pi y)dy$, and where

$$\mathcal{L}_L^{\pm}(v) = \pm\int_0^1 \frac{\partial u_{inc}}{\partial x}(\pm L, y)\bar{v}(\pm L, y)dy - \left\langle \mathbb{T}_L^{\pm}u_{inc}, v\right\rangle.$$

Finally, the problem is discretized by using a Galerkin approximation, replacing $H^1(B_L)$ by the finite-dimensional space of functions of the form

$$u(x,y) = \sum_{0\leq n\leq N_{trunc}}\ \sum_{0\leq p\leq P} U_{(n,p)}w_p(x)\cos(n\pi y)$$

Copyright © 2015 John Wiley & Sons, Ltd.

where the $w_p(x)$ forms a 1D finite element basis and N_{trunc} gives the number of modes kept in the expansion (always chosen greater than $N(k)$). In other words, we use a modal decomposition along y and finite elements along x.

4.3. *The fixed point algorithm*

Suppose $0 < k < \pi$. In that case, the user has to build a priori three shape functions h_0, $\hat{h}$ and $\check{h}$ satisfying (23). Then for a given $\varepsilon > 0$ and a given number of iterations *NITER*, the algorithm 1 produces a sequence of complex values of τ, which converges, for ε small enough to the unique solution of (24). The algorithm has to be run for various values of ε, to get the maximum value of ε for which the convergence holds.

Algorithm 1 Single-mode single-frequency invisibility up to a phase shift

$n = 1$
$\hat{\tau} = 0$
$\check{\tau} = 0$
if $n \leq NITER$ **then**
  Solve the scattering problem for the profile $y = 1 + \varepsilon h_0(x) + \varepsilon\hat{\tau}\hat{h}(x) + \varepsilon\check{\tau}\check{h}(x)$.
  return r_{00}^-
  $\hat{\tau} \leftarrow \hat{\tau} - \frac{1}{k\varepsilon}\Im m\left(r_{00}^-\right)$
  $\check{\tau} \leftarrow \check{\tau} + \frac{1}{k\varepsilon}\Re e\left(r_{00}^-\right)$
  $n \leftarrow n + 1$
end if
return $\hat{\tau}$, $\check{\tau}$ and r_{00}^-

More generally, Algorithms 2 and 3 correspond respectively to the multi-frequency (but single-mode) case and to the multi-modal case. Let us point out that contrary to the single-mode single-frequency case, all scattering values we want to cancel depend on all values of $\hat{\tau}$ and $\check{\tau}$. In particular, when the algorithm is convergent, some global norm of the vector of these scattering coefficients will decrease with n, but not necessarily each of them.

Algorithm 2 Single-mode multi-frequency invisibility up to a phase shift

$n = 1$
$\hat{\tau}_j = 0, j = 1, 2\cdots M$
$\check{\tau}_j = 0, j = 1, 2\cdots M$
if $n \leq NITER$ **then**
  Solve the scattering problem for the profile $y = 1 + \varepsilon\left(h_0(x) + \sum_{j=1}^{M}\hat{\tau}_j\hat{h}_j(x) + \sum_{j=1}^{M}\check{\tau}_j\check{h}_j(x)\right)$ at the frequencies $k_1, k_2, \cdots, k_M$.
  return $r_{00}^-(k_j), j = 1, 2\cdots M$
  for all $j = 1, 2\cdots M$ **do**
    $\hat{\tau}_j \leftarrow \hat{\tau}_j - \frac{1}{k_j\varepsilon}\Im m(r_{00}^-(k_j))$
    $\hat{\tau}_j \leftarrow \hat{\tau}_j + \frac{1}{k_j\varepsilon}\Re e(r_{00}^-(k_j))$
  end for
  $n \leftarrow n + 1$
end if
return $\hat{\tau}_j$, $\check{\tau}_j$ and $r_{00}^-(k_j)$ for $j = 1, 2\cdots M$

5. Numerical results

We present now some numerical results obtained in the single-mode case, for one or two frequencies. The method has been also validated in the case where $N(k) = 1$ (two propagative modes), but we do not present here the results because the fixed-point algorithm converges only for very small values of ε. We are currently working to improve the choice of the shape functions, in order to increase the limit value of ε for which the convergence holds.

5.1. *The single-mode case*

Let us begin with the single-mode case for one frequency $0 < k < \pi$. As explained previously, we first look for two even shape functions h_0 and $\hat{h}$ satisfying

$$\int_{\mathbb{R}} h_0(x)\cos(2kx)dx = 0 \text{ and } \int_{\mathbb{R}} \hat{h}(x)\cos(2kx)dx = 1.$$

Copyright © 2015 John Wiley & Sons, Ltd.

Algorithm 3 Multi-mode single-frequency 'invisibility'

$n = 1$
$\hat{\tau}^+_{mj} = 0, m = 0,\cdots,N(k), j = m,\cdots,N(k)$
$\check{\tau}^+_{mj} = 0, m = 0,\cdots,N(k), j = m,\cdots,N(k)$
$\hat{\tau}^-_{mj} = 0, m = 0,\cdots,N(k), j = m+1,\cdots,N(k)$
$\check{\tau}^-_{mj} = 0, m = 0,\cdots,N(k), j = m+1,\cdots,N(k)$
if $n \leq NITER$ **then**
Solve the scattering problem for the profile $y = 1+\varepsilon\left(h_0+\sum_{m=0}^{N(k)}\sum_{j=m}^{N(k)}\left(\hat{\tau}^+_{mj}\hat{h}^+_{mj}+\check{\tau}^+_{mj}\check{h}^+_{mj}\right)+\sum_{m=0}^{N(k)}\sum_{j=m+1}^{N(k)}\left(\hat{\tau}^-_{mj}\hat{h}^-_{mj}+\check{\tau}^-_{mj}\check{h}^-_{mj}\right)\right)$.
return $r^-_{mj}, m = 0,\cdots,N(k), j = m,\cdots,N(k)$, and $t^+_{mj},\cdots,N(k), j = m+1,\cdots,N(k)$
for all $m = 0,\cdots,N(k), j = m,\cdots,N(k)$ **do**
$\hat{\tau}^+_{mj} \leftarrow \hat{\tau}^+_{mj} - \mathfrak{Re}\left(\frac{1}{\alpha^+_{mj}\varepsilon}r^-_{mj}\right)$
$\check{\tau}^+_{mj} \leftarrow \check{\tau}^+_{mj} - \mathfrak{Im}\left(\frac{1}{\alpha^+_{mj}\varepsilon}r^-_{mj}\right)$
end for
for all $m = 0,\cdots,N(k), j = m+1,\cdots,N(k)$ **do**
$\hat{\tau}^-_{mj} \leftarrow \hat{\tau}^-_{mj} - \mathfrak{Re}\left(\frac{1}{\alpha^-_{mj}\varepsilon}t^+_{mj}\right)$
$\check{\tau}^-_{mj} \leftarrow \check{\tau}^-_{mj} - \mathfrak{Im}\left(\frac{1}{\alpha^-_{mj}\varepsilon}t^+_{mj}\right)$
end for
$n \leftarrow n+1$
end if
return $\hat{\tau}^+_{mj}, \check{\tau}^+_{mj}, r^-_{mj}, m = 0,\cdots,N(k), j = m,\cdots,N(k)$
return $\hat{\tau}^-_{mj}, \check{\tau}^-_{mj}, t^+_{mj}, m = 0,\cdots,N(k), j = m+1,\cdots,N(k)$

Once $\hat{h}$ is chosen, one can choose $\check{h}$ given by

$$\check{h}(x) = \hat{h}\left(x - \frac{\pi}{4k}\right),$$

which automatically satisfies

$$\int_{\mathbb{R}} \check{h}(x)\cos(2kx)dx = 0 \text{ and } \int_{\mathbb{R}} \check{h}(x)\sin(2kx)dx = 1.$$

Our first objective was to find a bump, which is invisible up to a phase shift. This led us to choose h_0 as follows:

$$h_0(x) = \left(\frac{x^2}{a^2}-1\right)^2 \chi_{\{|x|<a\}}(x), \tag{42}$$

where $a > 0$ is a parameter to be determined and $\chi_{\{|x|<a\}}$ is the characteristic function of the interval $]-a,a[$. Notice that the amplitude of h_0 is taken equal to 1, which is also the width of the waveguide. To find a, we have computed the function

$$a \to F(k,a) = \int_{-a}^{a}\left(\frac{x^2}{a^2}-1\right)^2\cos(2kx)dx.$$

Notice that $F(k,a) = 2a\mathcal{F}(h_0)(2ka)$ where $\mathcal{F}$ denotes the Fourier transform $\mathcal{F}(\phi)(\xi) = \int_{\mathbb{R}}\phi(x)e^{-i\xi x}dx$. As a consequence, we can easily check that

$$F(k,0) = 0 \text{ and } \lim_{a\to+\infty} F(k,a) = 0.$$

We see moreover on Figure 2 that $a \to F(k,a)$ is oscillating and vanishes for a sequence of values of a. For our experiments, we have taken the smallest value, which is approximatively given by $a = 1.8$. The corresponding h_0 function is represented in Figure 2.

We have used the same approach to build the function $\hat{h}$. But contrary to h_0, the amplitude of $\hat{h}$ cannot be fixed a priori. That is why we introduced another parameter η, looking for $\hat{h}$ of the form

$$\hat{h}(x) = \eta\left(\frac{x^2}{b^2}-1\right)^2\chi_{\{|x|<b\}}(x), \tag{43}$$

where the amplitude η and the width b must be fixed to satisfy $\int_{\mathbb{R}}\hat{h}(x)\cos(2kx)dx = 1$. It suffices to take b such that $F(k,b) \neq 0$ and η given by:

$$\eta = \frac{1}{F(k,b)}.$$

Copyright © 2015 John Wiley & Sons, Ltd.

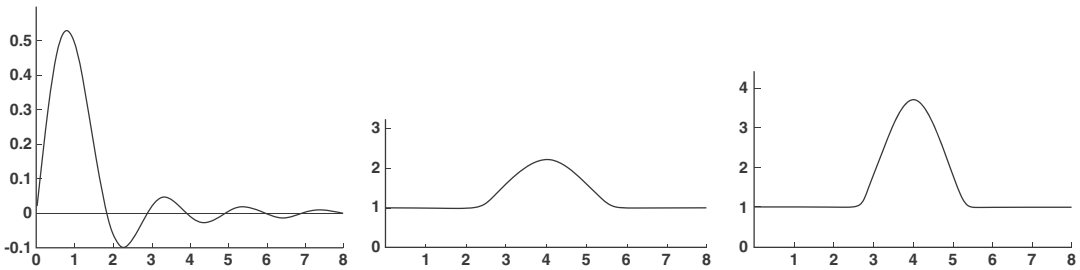

Figure 2. Left: the function $a \to F(k,a)$ for $k = \pi/2$, Middle: the bump-function h_0 for $a \sim 1.8$, Right: the bump-function $\hat{h}$ for $b \sim 1.5$.

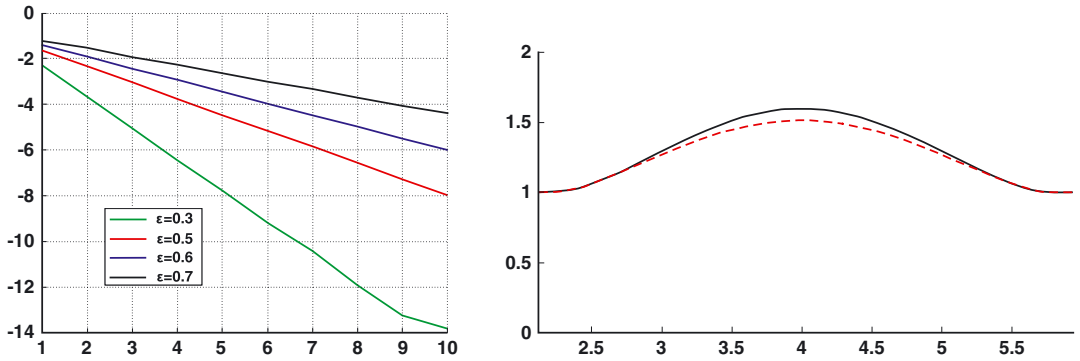

Figure 3. Left: $\log_{10}|r_{00}^-|$ as a function of the number of iterations n, Right: initial bump in continuous line, final bump in dashed line

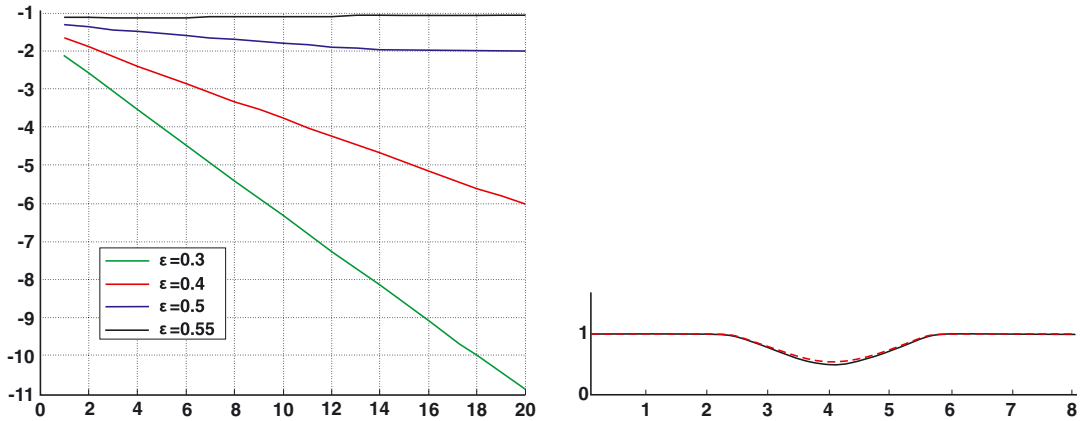

Figure 4. Left: $\log_{10}|r_{00}^-|$ as a function of the number of iterations n, Right: initial cavity in continuous line, final cavity in dashed line.

With the aforementioned choice for h_0, $\hat{h}$ and $\check{h}$ and for $k = \pi/2$, we observe that the fixed-point algorithm converges for any ε smaller than .7, which is quite large. It means that we find a bump of amplitude .7 which is invisible (up to a phase shift) at the frequency $k = \pi/2$. On Figure 3, we see the convergence history for different values of ε. First, for a given ε, we observe that the convergence is monotonic as expected for this algorithm. Moreover, we can check that the convergence becomes faster when ε decreases, which is coherent with the estimate (26). The final bump, in dashed line, is smaller than the initial one (associated to h_0). The correction produced by the function $\hat{\tau}\hat{h} + \check{\tau}\check{h}$ tends to diminish the perturbation.

The same experiment can be done by replacing h_0 by $-h_0$, in order to find a cavity, invisible up to a phase shift. The main difference that we observe on Figure 4 is that the divergence of the algorithm occurs earlier, that is for a value of ε around .5.

We have finally represented on Figure 5 the acoustic field in presence of an invisible bump/cavity. We observe that the field is an almost perfect plane wave at the left and at the right of the deformation. The result for the cavity can be used to build an invisible obstacle, inside the waveguide. Indeed, symmetrizing the result with respect to the axis $y = 1$, we get a symmetric obstacle in a waveguide of width 2, which is invisible up to a phase shift at the frequency $\pi/2$ (see Figure 6).

Let us finally mention that we can choose the shape functions h_0, $\hat{h}$ and $\check{h}$ in a similar way but such that the supports of $\hat{h}$ and $\check{h}$ do not intersect the support of h_0. This works again very well but the convergence history is more chaotic (see Figure 7).

Copyright © 2015 John Wiley & Sons, Ltd.

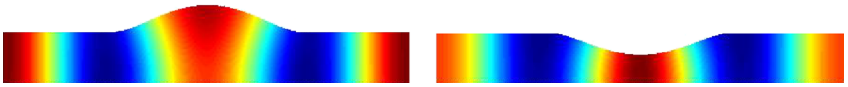

Figure 5. Left: $\Re(u)$ for the invisible bump, Right: $\Re(u)$ for the invisible cavity.

Figure 6. $\Re(u)$ for an invisible symmetric obstacle.

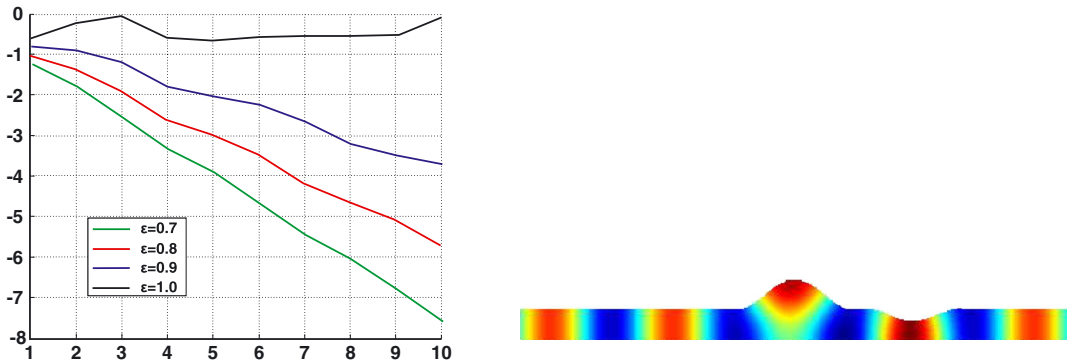

Figure 7. Left: $\log_{10}|r_{00}^-|$ as a function of the number of iterations n for shape functions with disjoint supports, Right: $Re(u)$ for the invisible deformation.

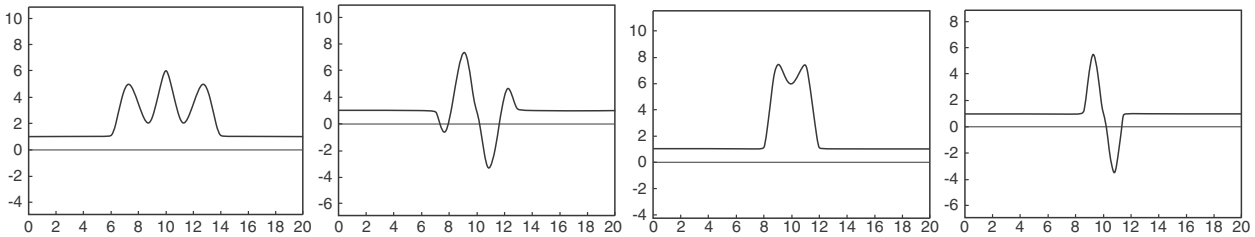

Figure 8. The shape functions $\hat{h}_1, \check{h}_1, \hat{h}_2, \check{h}_2$.

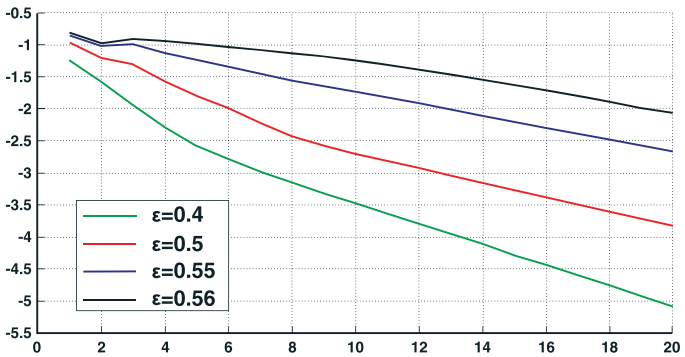

Figure 9. $\frac{1}{2}\log_{10}\left(|r_{00}^-(k_1)|^2 + |r_{00}^-(k_2)|^2\right)$ as a function of the number of iterations n.

Copyright © 2015 John Wiley & Sons, Ltd.

Figure 10. Left: initial cavity in continuous line, final cavity in dashed line, for $\varepsilon = .5$, Right: $Re(u)$ for the invisible deformation at the two frequencies k_1 and k_2.

5.2. The multi-frequency case

Now, we present some results for two frequencies $k_1 = 2\pi/3$ and $k_2 = 3\pi/4$ (which are smaller than π). Here, we have built even functions h_0, $\hat{h}_1$ and $\hat{h}_2$, and odd functions $\check{h}_1$ and $\check{h}_2$. Each function is a polynomial function on the positive part of its support $[0, L]$ and is globally of class $\mathcal{C}^1$. We observe on Figure 8 that we cannot avoid very large amplitudes and oscillations for the $\hat{h}_j$ and $\check{h}_j$. The width of the support of each function L is adapted manually to obtain acceptable functions. This phenomenon will become even more acute when the number of constraints will increase (in the multi-frequency or multi-modal cases), leading to shape functions $\hat{h}...$ and $\check{h}...$ with large oscillations and amplitude, which limits the range of ε for which the convergence holds.

We present the results for a function h_0 corresponding to a cavity (Figure 10). The convergence curves presented on Figure 9 correspond to the quantity $\frac{1}{2}\log_{10}\left(\left|r_{00}^{-}(k_1)\right|^2 + \left|r_{00}^{-}(k_2)\right|^2\right)$ as a function of the number of iterations of the fixed-point algorithm. We observe that the convergence is still ensured until ε around .6. However, the convergence is slowlier than in the single frequency case.

The obtained cavity for $\varepsilon = .5$, which is invisible up to a phase shift at the two frequencies $k_1 = 2\pi/3$ and $k_2 = 3\pi/4$ is presented on Figure 10.

References

1. Zolla F, Guenneau S, Nicolet A, Pendry J-B. Electromagnetic analysis of cylindrical invisibility cloaks and the mirage effect. *Optics Letters* 2007; **1;32**(9):1069–1071.
2. Popa B-I, Zigoneanu L, Cummer S-A. Experimental acoustic ground cloak in air. *Physical Review Letters* 2011; **106**:253901.
3. Farhat M, Enoch S, Guenneau S, Movchan AB. Broadband cylindrical cloak for linear surface waves in a fluid. *Physical Review Letters* 2008; **101**:134501.
4. Porter R, Newman J-N. Cloaking of a vertical cylinder in waves using variable bathymetry. *Journal of Fluid Mechanics* 2006; **750**:124–143.
5. Bonnet-Ben Dhia A-S, Nazarov SA, Taskinen J. *Underwater topography "invisible" for surface waves at given frequencies*. hal-01114632 2015.
6. Bonnet-Ben Dhia A-S, Nazarov S. Obstacles in acoustic waveguides becoming 'invisible' at given frequencies. *Acoustic Journal* 2013; **59**(6):633–639.
7. Pagneux V, Maurel A. Scattering matrix properties with evanescent modes for waveguides in fluids and solids. *The Journal of the Acoustical Society of America* 2004; **116**:1913–1920.
8. Maz'ya V, Nazarov S, Plamenevskij B. *Asymptotic Theory of Elliptic Boundary Value Problems in Singularly Perturbed Domains*, Vol. 1. Basel: Birkhäuser Verlag, 2000.
9. Nazarov S. Asymptotic expansions of eigenvalues in the continuous spectrum of a regularly perturbed quantum waveguide. *Theoretical and Mathematical Physics*; **167**(2):606–627.
10. Kress R. *Linear Integral Equations*. Springer-Verlag: Berlin, 1989.
11. Hazard C, Lunéville E. An improved multimodal approach for non uniform acoustic waveguides. *Journal of Applied Mathematics*; **73**(4):668–690.

Copyright © 2015 John Wiley & Sons, Ltd.